Received 10 January 2013
Revised 4 June 2013
Accepted 6 June 2013

Finite difference approach in porous media transport modeling for magnetohydrodynamic unsteady flow over a vertical plate

Darcian model

Sahin Ahmed
Department of Mathematics, Heat Transfer and Fluid Mechanics Research, Goalpara College, Assam, India
Abdul Batin
Department of Mathematics, Indira Gandhi College, Boitamari, Bongaigaon, Assam, India, and
Ali J. Chamkha
Manufacturing Engineering Department, The Public Authority for Applied Education and Training, Shuweikh, Kuwait

Abstract

Purpose – The purpose of this paper is to examine the effects of Darcian drag force and radiation-conduction on unsteady two-dimensional magnetohydrodynamic flow of viscous, electrically conducting and Newtonian fluid over a vertical plate adjacent to a Darcian regime in presence of thermal radiation and transversal magnetic field. A well-tested, numerically stable Crank-Nicolson finite-difference procedure is employed for the conservation equations. Excellent agreement is obtained for numerical solutions with previously published work.

Design/methodology/approach – In this investigation, an efficient, accurate, extensively validated and unconditionally stable finite-difference scheme based on the Crank-Nicolson model is developed to solve the governing coupled, non-linear partial differential equations. The accuracy and effectiveness of the method are demonstrated.

Findings – Different numerical results are obtained and presented graphically to explain the effect of various physical parameters on the velocity and temperature profiles, local, as well as average, skin friction and Nusselt number. It is found that, with a rise in Darcian drag force, flow velocity and temperature are reduced, but increased for all times. Both average and local skin frictions are reduced considerably with an increase in Darcian drag force, but reversed behavior is observed for the local Nusselt number. Increasing the thermal radiation effects accelerated the flow velocity as well as the fluid temperature and wall local skin friction in a saturated porous medium, but effectively reduced the local Nusselt number and average Nusselt number at the wall. Comparison with previously published works in the limits shows excellent agreement.

Research limitations/implications – The analysis is valid for unsteady, two-dimensional laminar flow of an optically thick no-gray gas, electrically conducting, and Newtonian fluid past an isothermal vertical surface adjacent to the Darcian regime with variable surface temperature. An extension to three-dimensional flow case is left for future work.

Practical implications – Practical interest of such study includes applications in electromagnetic lubrication, boundary cooling, bio-physical systems and in many branches of engineering and science. It is well known that the effect of thermal radiation is important in space technology and high temperature processes. Thermal radiation also plays an important role in controlling heat transfer process in polymer processing industry.

Keywords Lorentz force, Radiation heat flux, Darcian drag force, Eigenvalues, Maxwell's equations, Crank-Nicolson

Paper type Research paper

International Journal of Numerical Methods for Heat & Fluid Flow
Vol. 24 No. 5, 2014
pp. 1204-1223

0961-5539
DOI 10.1108/HFF-01-2013-0008

Nomenclature

(U,V)	dimensional velocity components in the X and Y directions, respectively (m s^{-1})
(u,v)	Velocity components along the distances x and y, respectively (m s^{-1})
$\bar{t}$	time (s)
g	acceleration due to gravity (m s^{-1})
β	coefficient of thermal expansion
T_W	temperature of the fluid at the plate (K)
T_∞	temperature of the fluid far away from the plate (K)
B_0	applied magnetic field
K_r	permeability of the porous medium
C_P	specific heat at constant pressure (J kg^{-1} K)
L	Characteristic length (m)
K_P^2	Darcian drag force coefficient (inverse permeability parameter)
M	Hartmann magnetohydrodynamic
F	conduction-radiation
Gr	free convection parameter
t	time (s)
Pr	Prandtl number
$\overline{B}$	magnetic induction intensity
$\overline{E}$	electric field intensity
$\bar{J}$	electric current density
$\bar{q}_r$	radiation heat flux
Ω	solid angle
$I_{b\lambda}$	spectral intensity for a black body
K_λ	absorption coefficient
Γ	Stefan-Boltzmann constant
G_λ	incident radiation
T_W	average value of the porous plate temperature
$e_{b\lambda}$	Plank's function
T	temperature of the fluid in the boundary layer
Nu_x	Local Nusselt number
$\overline{Nu}$	average Nusselt number

Greek symbols

β	coefficient of volume expansion for heat transfer (K^{-1})
v	fluid kinematic viscosity (m^2 s^{-1})
ρ	density (kg m^{-3}),
κ	thermal conductivity of fluid (W m^{-1} K^{-1})
θ	dimensionless temperature (K)
μ	magnetic permeability (Hm^{-1})
σ	electrical conductivity (VA^{-1} m^{-1})
τ_x	local skin friction
$\bar{\tau}$	average skin friction

Subscripts

w	conditions on the wall
∞	free stream conditions

1. Introduction

The study of MHD flow, through and across porous media, is of great theoretical interest because it has been applied to a variety of geophysical and astrophysical phenomena. Practical interest of such study includes applications in electromagnetic lubrication, boundary cooling, bio-physical systems and in many branches of engineering and science. In fact, flows of fluids through porous media have attracted the attention of a number of scholars because of their possible applications in many branches of science and technology. In fact a porous material containing the fluid is a non-homogeneous medium but it may be possible to treat it as a homogeneous one, for the sake of analysis, by taking its dynamical properties to be equal to the averages of the original non-homogeneous continuum. Thus a complicated problem of the flow through a porous medium gets reduced to the flow problem of a homogeneous fluid with some additional resistance. Heat transfer due to natural convection in a saturated with porous media is a new branch of thermo-fluid mechanics. The heat transfer phenomenon can be described by means of the hydrodynamics, the convective heat transfer mechanism and the electromagnetic field as they have a symbiotic relationship (Nield and Bejan, 2006; Vafai, 2005; Vadasz, 2008; Ingham and Pop, 1998). It is well known that the effect of thermal radiation is important in space technology and high temperature processes. Thermal radiation also plays an important role in controlling heat transfer process in polymer processing industry.

An early study was presented by Carrier and Greenspan (1960) who considered unsteady hydromagnetic flows past a semi-infinite flat plate moving impulsively in its own plane. Gupta (1960) considered unsteady magneto-convection under buoyancy forces. Pop (1969) reported on transient buoyancy-driven convective hydromagnetics from a vertical surface. Mohammadein *et al.* (1998) studied the radiative flux effects on free convection in Darcian porous media with the Rosseland model. Takhar *et al.* (2003) used shooting quadrature to analyze the mixed convection flow with thermal radiation effects in Darcy-Forchheimer porous media. More recently Chamkha *et al.* (2004) studied Rosseland radiation-conduction number effects on boundary layer wedge convection of a viscoelastic fluid in non-Darcian porous material. All of the above studies, however were for steady flows. The effect of unsteadiness in porous media and purely fluid regime convection is important in numerous energy and environmental systems. Several authors have therefore studied transient radiative-convective heat (and mass) transfer flows in pure fluids or porous media. Ganesan *et al.* (2001) studied theoretically the thermal radiation effects on unsteady flow past an impulsively started plate. Ghosh and Pop (2007) studied indirect radiation effects on convective gas flow. Raptis and Perdikis (2004) have also studied analytically the transient convection in a highly porous medium with unidirectional radiative flux. A three-dimensional Couette flow through a porous medium with heat transfer has also been investigated by Ahmed (2009). Ahmed and Zueco (2011) investigated the effects of Hall current, magnetic field, rotation of the channel and suction-injection on the oscillatory free convective MHD flow in a rotating vertical porous channel. Ahmed (2008) investigated the effect of transverse periodic permeability oscillating with time on the heat transfer flow of a viscous incompressible fluid through a highly porous medium bounded by an infinite vertical porous plate, by means of series solution method. Ahmed (2010) studied the effect of transverse periodic permeability oscillating with time on the free convective heat transfer flow of a viscous incompressible fluid through a highly porous medium bounded by an infinite vertical porous plate subjected to a periodic suction velocity.

The vast majority of radiation-convection flows have utilized algebraic flux approximations to simplify the general equations of radiative transfer (Siegel and Howell, 1993). The most popular of these simplifications remains the Rosseland diffusion approximation which has been employed by, for example, Ali *et al.* (1984) and later by Hossain *et al.* (1998). Radiation magnetohydrodynamic convection flows are also important in astrophysical and geophysical regimes. Raptis and Massalas (1998) considered induced magnetic field effects in their study of unsteady hydromagnetic-radiative free convection. More recent studies involving thermal radiation and transient hydromagnetic convection include the analyses by Prasad *et al.* (2006) which included species transfer and Zueco (2007) who also considered viscous heating. In numerous geophysical and metallurgical flows, porous media may also arise. Classically the Darcian model is used to simulate the bulk effects of porous materials on flow dynamics and is valid for Reynolds numbers based on the pore radius, up to approximately 10. Chamkha (1996) studied the transient free convection magnetohydrodynamic boundary layer flow in a fluid-saturated porous medium channel, and later Chamkha (2001) extended this study to consider the influence of temperature-dependent properties and inertial effects on the convection regime. Bég *et al.* (2005) presented perturbation solutions for the transient oscillatory hydromagnetic convection in a Darcian porous media with a heat source present. Takhar *et al.* (1996) studied the radiation effects on MHD free convection flow of a gas past a semi-infinite vertical plate. Thermal radiation and buoyancy effects on MHD free convective heat generating flow over an accelerating permeable surface with temperature-dependent viscosity has been studied by Seddeek (2001). Recently, Ghaly and Elbarbary (2002) have investigated the radiation effect on MHD free convection flow of a gas at a stretching surface with a uniform free stream. In all the above investigations, only steady-state flows over semi-infinite vertical plate have been studied. The unsteady free convection flows over vertical plate have been studied by Takhar *et al.* (1997), Muthucumaraswamy and Ganesan (1998). Chamkha *et al.* (2010) studied the effects of melting and thermal radiation on mixed convection from a vertical surface embedded in a non-Newtonian fluid saturated non-Darcy porous medium. Ahmed and Kalita (2013a) investigated the effects of porosity and magnetohydrodynamic on a horizontal channel flow of a viscous incompressible electrically conducting fluid through a porous medium in the presence of thermal radiation and transverse magnetic field. Ahmed and Kalita (2013a) presented the magnetohydrodynamic transient convective radiative heat transfer one-dimensional flow in an isotropic, homogenous porous regime adjacent to a hot vertical plate. Ahmed and Kalita (2013b) investigated the effects of chemical reaction as well as magnetic field on the heat and mass transfer of Newtonian two-dimensional flow over an infinite vertical oscillating plate with variable mass diffusion.

The purpose of the current investigation is to examine the effects of Darcian drag force and radiation-conduction on unsteady two-dimensional magnetohydrodynamic flow of viscous, electrically conducting and Newtonian fluid over a vertical plate adjacent to a Darcian regime in presence of thermal radiation and transversal magnetic field. A well-tested, numerically stable Crank-Nicolson finite-difference procedure is employed for the conservation equations. Excellent agreement is obtained for numerical methods with those of Takhar *et al.* (1997) and Abd El-Naby *et al.* (2003).

2. Mathematical formulae

Consider the unsteady flow of an electrically conducting viscous fluid adjacent to a vertical plate coinciding with the plane $Y=0$, where the flow is confined to $Y>0$. The vertical isothermal flat plate has been immersed in saturated Darcian regime. A uniform magnetic field of strength B_0 is imposed along the Y-axis (see Figure 1). MHD equations are the usual electromagnetic and hydrodynamic equations, but they are modified to take account of the interaction between the motion and the magnetic field. As in most problems involving conductors, Maxwell's displacement currents are ignored so that electric currents are regarded as flowing in closed circuits.

Assuming that the velocity of flow is too small compared to the velocity of light, that is, the relativistic effects are ignored, the system of Maxwell's equations can be written in the form (Roming, 1964):

$$\Delta \times \overline{B} = \mu \overline{J}, \quad \Delta . \overline{J} = 0, \quad \Delta \times \overline{E} = -\frac{\partial \overline{B}}{\partial \overline{t}}, \quad \Delta . \overline{B} = 0 \tag{1}$$

and Ohm's law can be written in the form:

$$\overline{J} = (\overline{E} + \overline{U} \times \overline{B}) \tag{2}$$

In the equation of motion, the body force $\overline{J} \times \overline{B}$ per unit volume is added. This body force represents the coupling between the magnetic field and the fluid motion which is called Lorentz force.

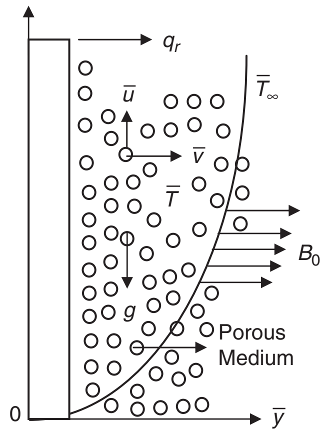

Figure 1.
Physical configuration and coordinate system

The induced magnetic field is neglected under the assumption that the magnetic Reynolds number is small. This is a rather important case for some practical engineering problems where the conductivity is not large in the absence of an externally applied field and with negligible effects of polarization of the ionized gas. It has been taken that $\overline{E} = 0$. That is, in the absence of convection outside the boundary layer, $\overline{B} = B_0$ and $\nabla \times \overline{B} = \mu \overline{J} = 0$, then (2) leads to $\overline{E} = 0$. Thus, the Lorentz force becomes $\overline{J} \times \overline{B} = \sigma(\overline{U} \times \overline{B}) \times \overline{B}$. In what follows, the induced magnetic field will be neglected. This is justified if the magnetic Reynolds number is small. Hence, to get a better degree of approximation, the Lorentz force can be replaced by $\sigma(\overline{U} \times B_0) \times B_0 = -\sigma B_0^2 \overline{U}$.

The radiating gas is said to be non-gray if its absorption coefficient is dependent on wave length (Shih, 1984). The equation that describes the conservation of radiative transfer in a unit volume for all wave length is:

$$\nabla.\bar{q}_r = \int_0^\infty K_\lambda(T)[4\pi I_{b\lambda}(T) - G_\lambda]\, d\lambda \tag{3}$$

and the incident radiation G_λ is defined as:

$$G_\lambda = \int_{\Omega=4\pi} I_{b\lambda}(\Omega) d\Omega \tag{4}$$

For an optically thin fluid exchanging radiation with an isothermal flat plate and according to (4) and Kirchhoff's law, the incident radiation is given by Cogley *et al.* (1968):

$$G_\lambda = 4\pi I_{b\lambda}(T_w) = 4e_{b\lambda}(T_w) \tag{5}$$

where T_w is the average value of the porous plate temperature. Then (3) reduces to:

$$\nabla.\bar{q}_r = 4 \int_0^\infty K_\lambda(T)[e_{b\lambda}(T) - e_{b\lambda}(T_w)] d\lambda \tag{6}$$

Expanding $e_{b\lambda}(T)$ and $K_\lambda(T)$ in Taylor series around T_w for small $(T-T_w)$ and substituting by the result in (6) reduces to:

$$\nabla.\bar{q}_r = -4\Gamma(T - T_w) \tag{7}$$

where:

$$\Gamma = \int_0^\infty K_{\lambda w}\left(\frac{\partial e_{b\lambda}}{\partial T}\right)_w d\lambda \tag{8}$$

$K_{\lambda w} = K_\lambda(T_w)$ is the mean absorption coefficient, $e_{b\lambda}$ is Plank's function, and T is the temperature of the fluid in the boundary layer.

Initially, it is assumed that the plate and the fluid are at the same temperature T_∞. At time $t \geqslant 0$, the plate temperature is assumed to vary with the power of the axial coordinate. It is also assumed that the fluid properties are constant except for the density variation that induces the buoyancy force.

Under the boundary layer and the Boussinesq approximations (Kakac and Yener, 1998; Rohsenow *et al.*, 1998), the unsteady two-dimensional laminar boundary layer free convective flow over a vertical plate adjacent to a Darcian regime is governed by the equations.

Equation of continuity:

$$\frac{\partial U}{\partial X} + \frac{\partial V}{\partial Y} = 0 \tag{9}$$

Equation of momentum:

$$\frac{\partial U}{\partial \bar{t}} + U\frac{\partial U}{\partial X} + V\frac{\partial U}{\partial Y} = g\beta(T - T_\infty) + v\frac{\partial^2 \bar{u}}{\partial \bar{y}^2} - \frac{\sigma}{\rho}B_0^2 U - \frac{v}{K_r}U \tag{10}$$

Equation of energy:

$$\frac{\partial T}{\partial \bar{t}} + U\frac{\partial T}{\partial X} + V\frac{\partial T}{\partial Y} = \frac{\kappa}{\rho\, Cp}\frac{\partial^2 t}{\partial Y^2} - 4\Gamma(T - T_w) \tag{11}$$

The initial and boundary conditions relevant to the problem are taken as:

$$\left.\begin{array}{l} \bar{t} \leqslant 0 : U = 0, V = 0, \quad T = T_\infty, \\ \bar{t} > 0 : U = 0, V = 0, \quad T = T_\infty + (T_W - T_\infty)X^m \text{ at } Y = 0 \\ U = 0, \quad T = T_\infty \quad \text{at } X = 0 \\ U \to 0, \quad T \to T_\infty \quad \text{at } Y \to \infty \end{array}\right\} \tag{12}$$

On introducing the following non-dimensional quantities:

$$\left.\begin{array}{l} x = \frac{X}{L}, \quad y = \frac{Y}{L}Gr^{\frac{1}{4}}, \quad u = \frac{UL}{v}Gr^{-\frac{1}{2}}, \quad v = \frac{VL}{v}Gr^{-\frac{1}{4}}, \\ t = \frac{v\bar{t}}{L^2}Gr^{1/2}, \ \theta = \frac{T-T_\infty}{T_w-T_\infty}, \ Pr = \frac{\rho v Cp}{\kappa}, \ Gr = \frac{g\beta L^3(T_w-T_\infty)}{v^2}, \\ F = \frac{4\Gamma L^2}{vGr^{1/2}}, \quad K_p^2 = \frac{Gr^{1/2}}{K_r L^2}, \quad M = \frac{\sigma L^2 B_0^2}{\mu Gr^{1/2}} \end{array}\right\} \tag{13}$$

Equations (9)-(11) are reduced to the following non-dimensional form:

$$\frac{\partial u}{\partial x} + \frac{\partial v}{\partial y} = 0 \tag{14}$$

$$\frac{\partial u}{\partial t} + u\frac{\partial u}{\partial x} + v\frac{\partial u}{\partial y} = \theta + \frac{\partial^2 u}{\partial y^2} - (M + K_P^2)u \tag{15}$$

$$\frac{\partial \theta}{\partial t} + u\frac{\partial \theta}{\partial x} + v\frac{\partial \theta}{\partial y} = \frac{1}{Pr}\frac{\partial^2 \theta}{\partial y^2} - F(\theta - 1) \tag{16}$$

The corresponding initial and boundary conditions in non-dimensional form are:

$$\left.\begin{array}{llll} t \leqslant 0: u = 0, & v = 0, & \theta = 0 & \\ t > 0: u = 0, & v = 0, & \theta = x^n & \text{at} \quad y = 0 \\ u = 0, & \theta = 0 & & \text{at} \quad x = 0 \\ u \to 0, & \theta \to 0 & & \text{as} \quad y \to \infty \end{array}\right\} \tag{17}$$

We note that the optically thick radiative approximation is valid for relatively low values of the parameter, F. In the present study, we shall consider the supplementary influence of transverse magnetic field for the case where the fluid is saturated with air for which the Prandtl number is assumed to take the value 0.7.

3. Solution methodology

The unsteady, non-linear coupled equations (Ahmed 2008, 2009; Ahmed and Zueco, 2011) with conditions (17) are solved by using an implicit finite-difference scheme which is discussed by Soundalgekar (1981). Consider a rectangular region with x varying from 0 to 1 and y varying from 0 to $y_{max}(=6.4)$, where y_{max} corresponds to $y = \infty$ at which lies well outside the momentum and energy boundary layers. The region to be examined in (x,y,t) space is covered by a rectilinear grid with sides parallel to axes with Δx, Δy and Δt, the grid spacing in x, y and t directions, respectively. The grid points (x,y,t) are given by $(i\Delta x,\ j\Delta y,\ n\Delta t)$, where $i = 0(1)P$, $j = 0(1)Q$, $\Delta x = 1/P$, $\Delta y = y_{max}/Q$ and $n = 0,1,2,\ldots$. The grid sizes are taken as $\Delta x = 1/16$, $\Delta y = 0.2$ and $\Delta t = 0.05$. The functions satisfying the difference equations at the grid point are $u_{i,j}^n$, $v_{i,j}^n$, and $\theta_{i,j}^n$. The finite-difference equations (14) to (16) are given by:

$$\frac{[u_{i,j}^{n+1} - u_{i-1,j}^{n+1} + u_{i,j}^n - u_{i-1,j}^n - u_{i-1,j-1}^{n+1} + u_{i,j-1}^n - u_{i-1,j-1}^n]}{4\Delta x} + \frac{[v_{i,j}^{n+1} - v_{i-1,j}^{n+1} + v_{i,j}^n - u_{i,j-1}^n]}{2\Delta \text{y}} = 0 \tag{18}$$

$$\frac{[u_{i,j}^{n+1} - u_{i,j}^n]}{\Delta \text{t}} + u_{i,j}^n\frac{[u_{i,j}^{n+1} - u_{i-1,j}^{n+1} + u_{i,j}^n - u_{i-1,j}^n]}{2\Delta x} + v_{i,j}^n\frac{[u_{i,j+1}^{n+1} - u_{i,j-1}^{n+1} + u_{i,j+1}^n - u_{i,j-1}^n]}{4\Delta \text{y}}$$
$$= \frac{[\theta_{i,j}^{n+1} + \theta_{i,j}^n]}{2} + \frac{1}{2(\Delta \text{y})^2}[u_{i,j-1}^{n+1} - 2u_{i,j}^{n+1} + u_{i,j+1}^{n+1} + u_{i,j-1}^n - 2u_{i,j}^n + u_{i,j+1}^n]$$
$$- \frac{1}{2}(M + K^{-1})[u_{i,j}^{n+1} + u_{i,j}^n] \tag{19}$$

$$\frac{[\theta_{i,j}^{n+1}-\theta_{i,j}^{n}]}{\Delta \mathrm{t}}+u_{i,j}^{n}\frac{[\theta_{i,j}^{n+1}-\theta_{i-1,j}^{n+1}+\theta_{i,j}^{n}-\theta_{i-1,j}^{n}]}{2\Delta x}+v_{i,j}^{n}\frac{[\theta_{i,j+1}^{n+1}-\theta_{i,j-1}^{n+1}+\theta_{i,j+1}^{n}-\theta_{i,j-1}^{n}]}{4\Delta \mathrm{y}}$$
$$=\frac{[\theta_{i,j-1}^{n+1}-2\theta_{i,j}^{n+1}+\theta_{i,j+1}^{n+1}+\theta_{i,j-1}^{n}-2\theta_{i,j}^{n}+\theta_{i,j+1}^{n}]}{2Pr(\Delta \mathrm{y})^{2}}-F\frac{[(\theta_{i,j}^{n+1}+\theta_{i,j}^{n})-1]}{2} \tag{20}$$

The coefficient appearing in difference equations are treated as constants. The finite-difference equations at every internal nodal point on a particular n-level constitute a tridiagonal system of equations. These equations are solved by using the Thomas algorithm (Hoffman, 1992). Computations are carried out until the steady-state solution is assumed to have been reached when the absolute difference between the values of velocity as well as temperature at two consecutive time steps are $<10^{-5}$ at all grid points.

3.1 Stability analysis

The stability analysis of the finite-difference equations that approximates the solution of heat transfer problems has been studied by Soundalgekar (1981) and Muthucumaraswamy and Ganesan (1998). In this section, the von Neumann method is used to study the stability condition for the finite difference (18), (19) and (20).

The Fourier expansions for u and θ are given by:

$$\begin{aligned} u &= \Phi(t)exp(I\alpha x)\,exp\,(I\eta y)\\ \theta &= \Psi(\mathrm{t})exp(I\alpha x)\,exp\,(I\eta y)\end{aligned} \tag{21}$$

where $I=\sqrt{-1}$. Substituting from (21) in (19) and (20). Under the assumptions that coefficients u and θ are constant over any one step and denoting the values after one time step by Φ' and Ψ', we may get that, after simplification:

$$\begin{aligned}&\frac{\Phi'-\Phi}{\Delta t}+\frac{u(\Phi'-\Phi)[1-exp(-I\alpha\Delta x)]}{2\Delta x}+\frac{v(\Phi'+\Phi)I\sin(\beta\Delta y)}{2\Delta y}\\ &=\frac{(\Psi'+\Psi)}{2}-(M+K^{-1})\frac{(\Phi'+\Phi)}{2}+\frac{(\Phi'+\Phi)[\cos(\eta\Delta y)-1]}{(\Delta y)^{2}}\end{aligned} \tag{22}$$

$$\begin{aligned}&\frac{\Psi'-\Psi}{\Delta t}+\frac{u(\Psi'-\Psi)[1-exp(-I\alpha\Delta x)]}{2\Delta x}+\frac{v(\Psi'+\Psi)I\sin(\eta\Delta y)}{2\Delta y}\\ &=\frac{(\Psi'+\Psi)[\cos(\eta\Delta y)-1]}{pr(\Delta y)^{2}}-F\left[\frac{\Psi'+\Psi}{2}-1\right]\end{aligned} \tag{23}$$

Equations (23)-(25) can be rewritten as:

$$(1+A)\Phi'=(1-A)\Phi+\frac{\Delta t}{2}[\Psi'+\Psi] \tag{24}$$

$$(1+B)\Psi'=(1-B)\Psi+F\Delta t \tag{25}$$

where:

$$A = \frac{u}{2}\frac{\Delta t}{\Delta x}[1 - exp(-I\alpha\Delta x)] + \frac{v}{2}\frac{\Delta t}{\Delta y}I\sin(\eta\Delta y) - [\cos(\eta\Delta y) - 1]\frac{\Delta t}{Pr(\Delta y)^2} + \frac{\Delta t}{2}(M + K^{-1})$$

$$B = \frac{u}{2}\frac{\Delta t}{\Delta x}[1 - exp(-I\alpha\Delta x)] + \frac{v}{2}\frac{\Delta t}{\Delta y}I\sin(\eta\Delta y) - [\cos(\eta\Delta y) - 1]\frac{\Delta t}{Pr(\Delta y)^2}$$

Equations (26)-(28) can be written in matrix form as follows:

$$\begin{pmatrix} \Phi' \\ \Psi' \end{pmatrix} = \begin{pmatrix} \frac{1-A}{1+A} & \frac{\Delta t}{(1+A)(1+B)} \\ 0 & \frac{1-B}{1+B} \end{pmatrix} \begin{pmatrix} \Phi \\ \Psi \end{pmatrix} + \begin{pmatrix} \frac{F\Delta t^2}{2(1+A)(1+B)} \\ \frac{F\Delta t}{(1+B)} \end{pmatrix} \tag{26}$$

Now, for stability of the finite-difference scheme, the modulus of each eigenvalue of the amplification matrix does not exceed unity. Since the matrix Equation (26) is triangular, the eigenvalues are its diagonal elements. The eigenvalues of the amplification matrix are $(1-A)/(1+A)$ and $(1-B)/(1+B)$. Assuming that, u is everywhere non-negative and v is everywhere non-positive, we get:

$$A = 2a\,sin^2\left(\frac{\alpha\Delta x}{2}\right) + 2c\,sin^2\left(\frac{\eta\Delta y}{2}\right) + I[a\sin(\alpha\Delta x) - b\sin(\eta\Delta y)] + \frac{\Delta t}{2}(M + K^{-1})$$

$$a = \frac{u}{2}\frac{\Delta t}{\Delta x}, \quad b = \frac{|v|}{2}\frac{\Delta t}{\Delta y}, \quad c = \frac{\Delta t}{(\Delta y)^2}$$

Since the real part of $A \geqslant 0$, $|(1-A)/(1+A)| \leqslant 1$ always. Similarly, $|(1-B)/(1+B)| \leqslant 1$. Hence, the finite-difference scheme is unconditionally stable. The local truncation error is $O(\Delta t^2 + \Delta y^2 + \Delta x)$ and it tends to zero as Δt, Δx and Δy tend to zero. Hence, the scheme is compatible. Stability and compatibility ensures convergence (Hoffman, 1992).

4. The local skin friction and heat transfer

Knowing the velocity and temperature profiles, it is customary to study skin friction and Nusselt number in their transient and steady-state conditions.

The local, as well as average, skin friction and Nusselt number in terms of dimensionless quantities are given by Takhar *et al.* (1997):

$$\begin{aligned} \tau_x &= Gr^{3/4}\frac{\partial u}{\partial y}\bigg|_{y=0} \\ \bar{\tau} &= Gr^{3/4}\int_0^1 \frac{\partial u}{\partial y}\bigg|_{y=0} dx \\ Nu_x &= -\frac{xGr^{1/4}}{\theta|_{y=0}}\frac{\partial \theta}{\partial y}\bigg|_{y=0} \\ \overline{Nu} &= -Gr^{1/4}\int_0^1 \frac{\frac{\partial \theta}{\partial y}\big|_{y=0}}{\theta|_{y=0}} dx \end{aligned} \tag{27}$$

The derivatives involved in (27) are evaluated using the following five-point approximation formula:

$$\left.\frac{\partial u}{\partial y}\right|_{y=0} = \frac{-17u_{i,0}^{n} + 24u_{i,1}^{n} - 12u_{i,2}^{n} - u_{i-1,j}^{n} + 8u_{i,3}^{n} - 3u_{i,4}^{n}}{12\Delta y} \tag{28}$$

and integrals are evaluated using Newton cotes formula.

5. Accuracy

To test the validity of numerical Crank-Nicolson computations, our results for steady-state values of the velocity was compared to those of the curves computed by Takhar *et al.* (1997). These are plotted in Table I. It was observed that our results agree very well with those of Takhar *et al.* (1997).

Also we have obtained a comprehensive range of solutions to the transformed conservation equations. We have compared the flow velocity distributions in Table II to those of the curves computed by Abd El-Naby *et al.* (2003). It is clearly seen from Table II that the results are in excellent agreement. As the accuracy of the numerical solutions is very good, the values of u corresponding to numerical solutions are very close to each other. With increasing Pr in Table II, there is a clear decrease in velocity, i.e. the flow is decelerated through the boundary layer transverse to the plate. Pr encapsulates the ratio of momentum diffusivity to thermal diffusivity for a given fluid. It is also the product of dynamic viscosity and specific heat capacity divided by thermal conductivity. Higher Pr fluids will therefore posses higher viscosities (and lower thermal conductivities) implying that such fluids will flow slower than lower Pr fluids. As a result the velocity will be decreased substantially with increasing Prandtl number.

	Takhar *et al.* (1997)			Present work		
y	$x=0.1$	$x=0.5$	$x=1.0$	$x=0.1$	$x=0.5$	$x=1.0$
0	0.00000	0.00000	0.00000	0.00000	0.00000	0.00000
2	0.14925	0.36507	0.53510	0.14931	0.36509	0.53513
4	0.04227	0.15372	0.26202	0.04229	0.15375	0.26210
6	0.00731	0.03915	0.07618	0.00727	0.03916	0.07617
8	0.00136	0.00741	0.01225	0.00135	0.00743	0.01230
10	0.00000	0.00000	0.00000	0.00000	0.00000	0.00000

Table I. Comparison of steady-state velocity profiles (u) for the present results with Takhar *et al.* (1997) for $K_p=0$, $F=0$, $M=0$, $t=0.5$, $Pr=0.7$ and $m=0$

	Abd El-Naby *et al.* (2003)			Present work		
y	$Pr=0.7$	$Pr=1$	$Pr=1.5$	$Pr=0.7$	$Pr=1$	$Pr=1.5$
0	0.00000	0.00000	0.00000	0.00000	0.00000	0.00000
2	4.85912	4.25143	3.72483	4.85920	4.25147	3.72486
4	1.43471	1.03526	0.75277	1.43475	1.03532	0.75281
6	0.35270	0.18907	0.07892	0.35281	0.18913	0.07897
8	0.07315	0.04301	0.03170	0.07318	0.04320	0.03175
10	0.03502	0.02162	0.01170	0.03515	0.02171	0.01183

Table II. Comparison of steady-state velocity profiles (u) for the present results with Abd El-Naby *et al.* (2003) for $K_p=0$, $F=0.05$, $M=5.0$, $t=2.5$, $x=1$ and $m=1$

6. Results and discussions

To gain a perspective of the physics of the flow regime, we have numerically evaluated the effects of Hartmann number (*M*), Darcian drag force (K_P^2), radiation-conduction parameter (F), dimensionless time (*t*) on the velocity (*u*), temperature (*θ*), average and local skin frictions ($\bar{\tau}/Gr^{3/4}, \tau_x/Gr^{3/4}$) as well as Nusselt ($\overline{Nu}/Gr^{1/4}, Nu_x/Gr^{1/4}$) numbers. Here we consider the Prandtl number *Pr* is taken for air at 20°C ($Pr = 0.71$). To ascertain the accuracy of the numerical results, the present study is compared with the previous study. The velocity profiles are compared with the available solutions of Takhar *et al.* (1997) and Abd El-Naby *et al.* (2003). It is observed that the present results are in good agreement with those of Takhar *et al.* (1997) and Abd El-Naby *et al.* (2003).

Spatial velocity (*u*) distributions, for two time values are illustrated in Figure 2, for the effect of Hartmann hydromagnetic parameter (*M*). This parameter represents the ratio of the hydromagnetic retarding force to the viscous hydrodynamic force in the boundary layer. The classical velocity overshoot is identified [5,6,7,37] near the stationary plate surface for lower values of *M* that is, 1.0 and 5.0; with $M = 10.0$ this overshoot is clearly suppressed owing to stronger resistance to the flow. We note that for $t = 1.5$, the profiles are always greater in value than for $t = 0.5$ that is, the flow is accelerated considerably with time, although velocities are strongly reduced with an increase in Hartmann number. We observe that an increase in Hartmann number (*M*) from 1.0 through 5-10 (strong magnetic flux density) causes a significant decrease in the flow velocity, *u* with distance normal to the plate surface into the boundary layer (*y*). This trend is consistent with many classical studies on magneto-convection showing that the hydromagnetic body force retards the flow that is, decelerates the fluid causing a thinning in the boundary layer thickness. Very high Hartmann numbers (i.e. $M \gg 1$) are usually associated with the formation of a Hartmann boundary layer (Shercliff, 1965). All profiles decrease toward zero in the free stream, although this state is attained much faster for higher magnetic field values ($M = 10$) and for shorter times.

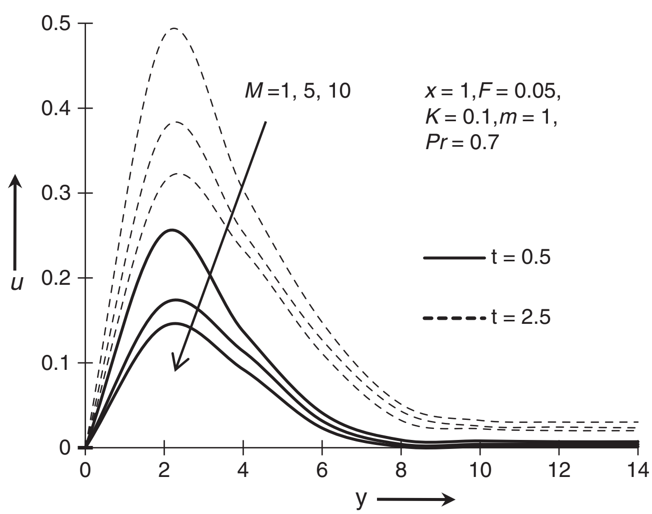

Figure 2.
Spatial velocity distribution (u) for the effect of Hartmann hydromagnetic parameter

In Figure 3, the dimensionless average skin friction profiles ($\bar{\tau}/Gr^{3/4}$) in time for different Hartmann numbers (M) are illustrated. A strong decrease is observed in average Skin friction from $t=0$ to $t=1$ after which profiles, although they continue to decrease with increasing M values, tend for $M = 0,5,10,15$ and 20, to the steady state. For these values of Hartmann number, profiles are always positive indicating that flow reversal does not occur. After $t>0.6$, the average skin friction becomes a constant function of Hartmann number and time parameter.

In Figure 4, average Nusselt number profiles ($\overline{Nu}/Gr^{1/4}$) in time for the influence of radiation-conduction parameter (F) are presented. In all cases, profiles are a maximum initially at the isothermal plate and decay quickly from the wall with time. An increase in F from 0.0 through 0.02, 0.04 to 0.08 is seen to markedly reduce average Nusselt number especially at shorter times ($0.2<t<0.4$); with further elapse of time all profiles converge that is, radiation effects are negligible for large times. Increasing F implies a greater augmentation of heat transfer by thermal radiation which will serve to increase fluid temperatures in the regime; the average Nusselt number at the wall will therefore be reduced as greater thermal energy (heat) will be imparted to the fluid-saturated regime raising temperatures within the porous regime. However, the values of $\overline{Nu}/Gr^{1/4}$ gradually descend up to the time $t=0.6$, and when $t>0.6$ the profiles of $\overline{Nu}/Gr^{1/4}$ become linear, i.e. become a constant function of conduction-radiation and time.

In Figure 5, the influence of the Darcian drag force parameter (K_P) on the time evolution of average skin friction profiles ($\bar{\tau}/Gr^{3/4}$), is depicted. As K_P increases from 0.1 through 0.5, 1, 1.5 to 2, a very large escalation in Darcian drag force is caused, as expressed in (15) in the linear term, $-K_P^2$, which decelerates the flow and reduces the average skin friction at the plate. Steady-state values are achieved faster with lower Darcian drag ($K_P=0.1$) than with higher Darcian drag ($K_P=2$). Moreover, the values of $\bar{\tau}/Gr^{3/4}$ gradually escalated up to the time $t = 0.6$, and when $t > 0.6$ the profiles of $\bar{\tau}/Gr^{3/4}$ become linear.

In Figure 6, the combined effects of time (t) and radiation-conduction parameter (F) on spatial distribution of temperature (θ) through the boundary layer is shown.

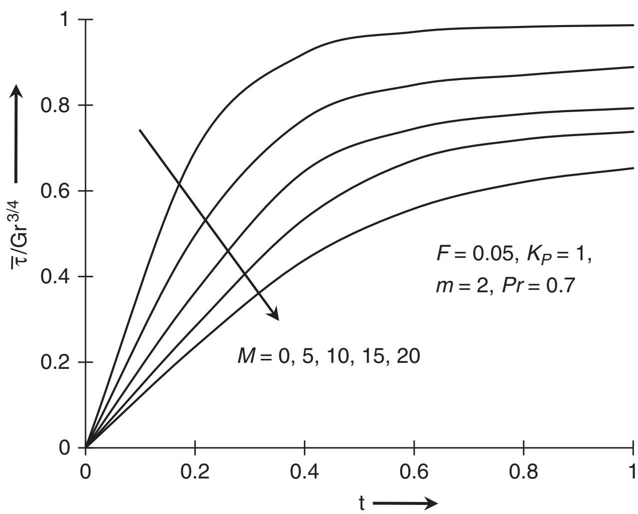

Figure 3.
Average skin friction distribution for the effect of Hartmann hydromagnetic parameter

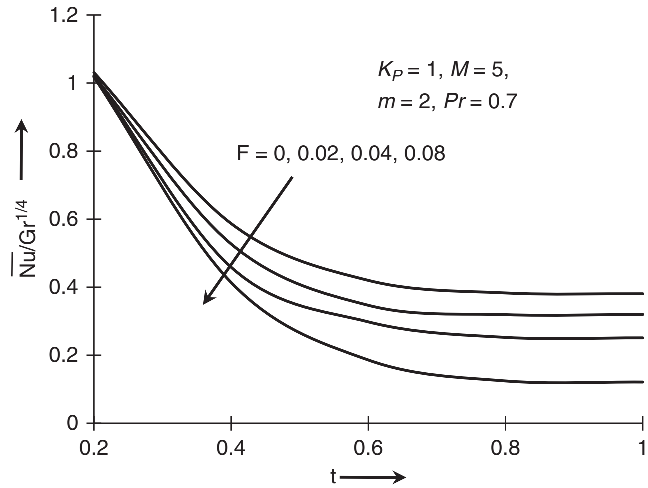

Figure 4.
The effect of radiation-conduction parameter on average Nusselt number against time

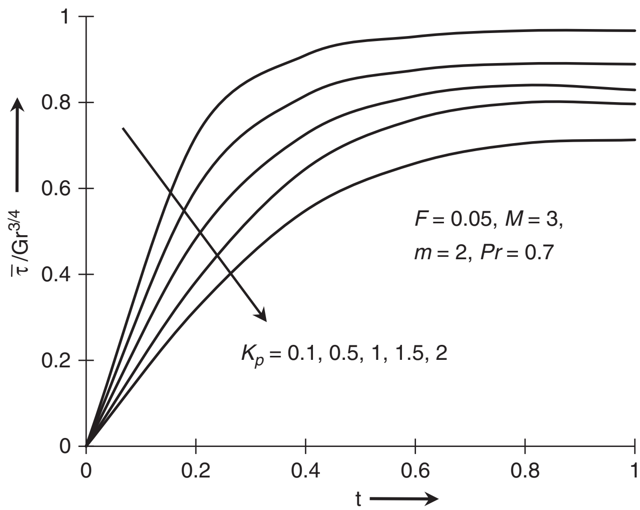

Figure 5.
Average skin friction distribution for the effect of porosity parameter against time

An increase in F serves to supplement fluid thermal conductivity with radiation contribution and significantly heats the fluid-saturated regime that is, increases temperature values. Similar results were reported by Ali *et al.* (1984), Hossain *et al.* (1998) and very recently by Ghosh and Bég (2008). A large difference is observed between the profiles computed at $t = 0.5$ and $t = 1.5$, indicating that thermal radiation effects are amplified at greater times, compared with smaller times where the flow is still developing. After greater times, a greater quantity of thermal energy will be absorbed into the fluid regime via the imposed flux causing enhanced heating of the fluid. For example, for $t = 1.5$, at $y = 2$, for $F = 0.05$ (maximum thermal radiation effect), θ reaches a value of approximately 0.51, whereas the corresponding value for $t = 0.5$ is much lower at $F = 0.23$.

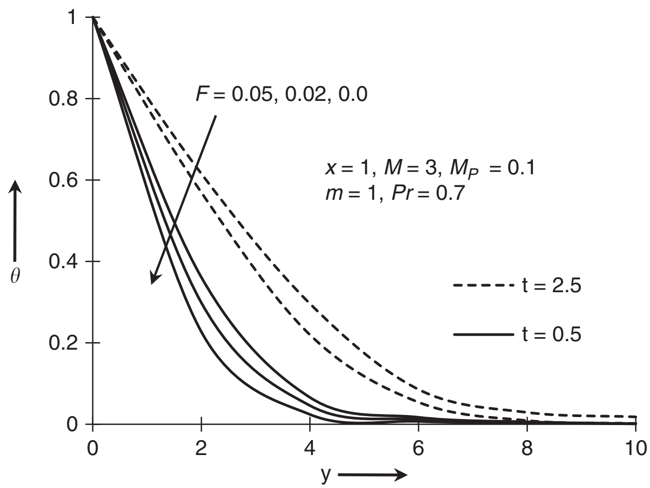

Figure 6.
Spatial temperature distribution (θ) for the effect of radiation-conduction parameter (F) at $t = 0.5$ and $t = 2.5$

In Figure 7 we have plotted the spatial variation of velocity for the combined effects of radiation-conduction parameter (F) and time (t). Again a velocity overshoot is observed in the close vicinity of the plate; however, this overshoot is distinctly greater for the highest value of $F\,(=0.05)$ and greater time values ($t = 2.5$); all profiles descend gradually to zero far from the wall. Thermal radiation therefore augments the flow that is, accelerates the flow in the porous regime. Velocities are minimized when thermal conduction swamps thermal radiation that is, for $F = 0.1$.

The effect of temperature exponent (m) at $t = 0.5$ and $t = 2.5$ on the flow velocity (u) is shown in Figure 8. For $m = 0$ the power-law variation of temperature at the plate surface reduces from $T = T_\infty + (T_W - T_\infty)X^m$ to $T = T_\infty$ i.e. we obtain an isothermal scenario (constant wall temperature). With an increase in m from 2.0 to 3.0 (non-iso-thermo case), the velocity is increased in the boundary layer. As such

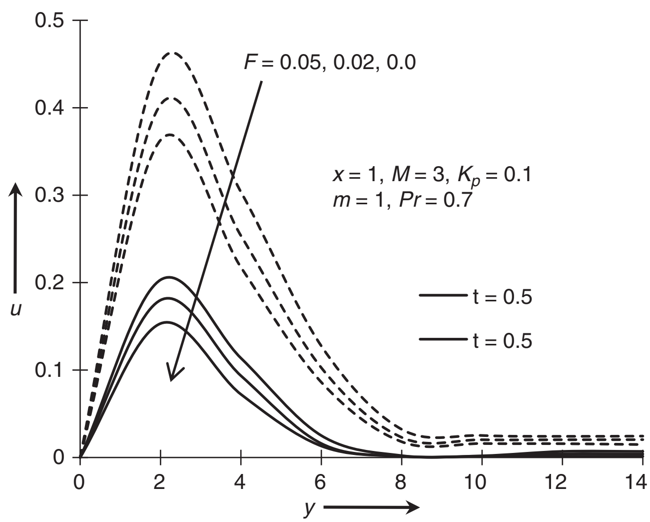

Figure 7.
Spatial velocity distribution (u) for the effect of radiation-conduction parameter (F)

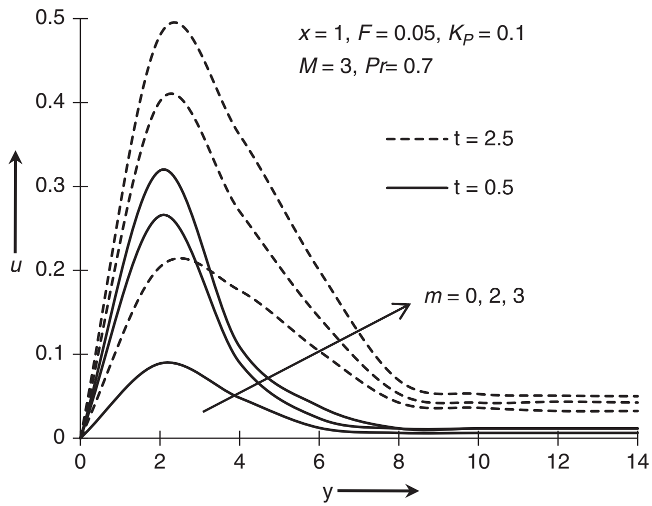

Figure 8.
Spatial velocity distribution (u) for the effect of temperature exponent (m)

increasing power-law exponents in the plate surface temperature variations serve to accelerate the flow in the boundary layer. Here velocity overshoot has been observed at $t = 2.5$ and $m = 3$.

Figures 9 and 10 illustrate the influence of the inverse permeability parameter (K_P) on the boundary layer variables, u and θ, respectively at $t = 0.5$ and $t = 2.5$. The parameter K_P as defined in Equation (15) is inversely proportional to the actual permeability, K, of the porous medium. The Darcian drag force in the momentum equation, namely, $(-K_P^2 u)$, is therefore directly proportional to K_P. An increase in K_P will therefore increase the resistance of the porous medium (as the permeability physically becomes less with increasing K) which will serve to decelerate the flow and reduce velocity, u. This trend is indeed maintained with further separation from the plate. Deceleration of the flow is therefore sustained at considerable distance from the plate toward the free stream as inverse permeability (K_P) parameter is increased. The profiles of flow velocity decay monotonically for all values of K_P from the

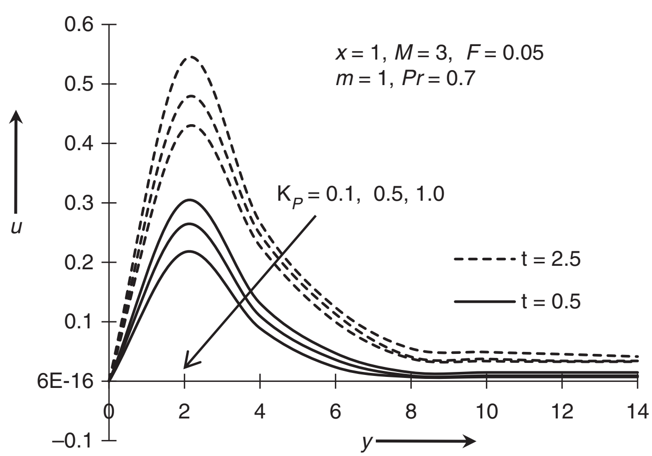

Figure 9.
Spatial velocity distribution (u) for the effect of Darcian drag force (K_P) at $t = 0.5$ and $t = 2.5$

maximum value of u at $y = 2$ to the minimum value of u in the free stream. This effect is accentuated close to the surface where a peak in the velocity profile arises. With further distance transverse to the surface, the velocity profiles are all found to decay into the free stream. For increasing K_P values, the time t required to attain the steady-state scenario is also elevated considerably. As such, the steady state is achieved faster for higher values of K_P. On the other hand, with increasing K_P values, the temperature profile (Figure 2(b)) in the regime is found to be decreases, i.e. the boundary layer is cooled. A reduction in the volume of solid particles in the medium implies a lower contribution via thermal conduction. This serves to decrease the fluid temperature.

In Figure 11, the effects of the radiation-conduction (F) and Darcian drag force (K_P) on the local skin friction ($\tau_x/Gr^{3/4}$) are shown for different values of x. Increasing F

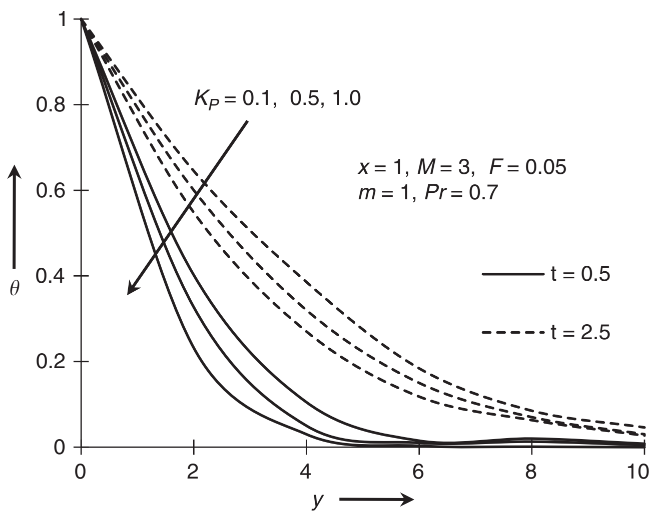

Figure 10. Spatial temperature distribution (θ) for the effect of Darcian drag force (K_P) at $t = 0.5$ and $t = 2.5$

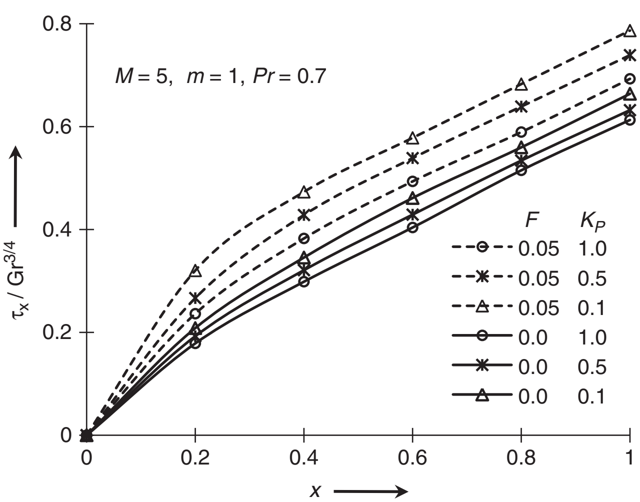

Figure 11. The effect of radiation-conduction and Darcian drag force on local skin friction

strongly boosts the flow and increases, $(\tau_x/Gr^{3/4})$, profile values which remain positive for all x and indicating that backflow does not occur; however, with increasing of K_P from 0.1 through 0.5-1.0, the local skin friction descend. Moreover, all the profiles of $(\tau_x/Gr^{3/4})$ are also ascend with increasing x.

In Figure 12, an increase in Darcian drag force K_P from 0.1 through 0.5-1.0 is observed to enhance the local Nusselt number $(Nu_x/Gr^{1/4})$. Conversely, the local Nusselt number is depressed by the effects of radiation-conduction (F) from 0.0 to 0.05. The values of, $Nu_x/Gr^{1/4}$ are continuously increased with increasing values of x.

7. Conclusions

A numerical solution is developed using an efficient, accurate, extensively validated and unconditionally stable implicit finite-difference scheme of the Crank-Nicolson type for the transient hydromagnetic convective heat transfer in boundary layer flow over a semi-infinite vertical plate adjacent to a Darcian porous regime in the presence of thermal radiation and Darcian drag force effects. A flux model is employed to simulate thermal radiation effects. From the present numerical investigation the following conclusions may be drawn:

- The classical velocity overshoot is detected close to the plate surface for low to intermediate values of M at both small and large times; however this overshoot vanishes for larger strengths of the transverse magnetic field $(M = 10)$.
- The decrease of temperature may be attributed to the loss of heat energy due to radiation as well as low diffusion.
- An increase in the Lorentz force with the presence of the Darcian resistance reduces the skin friction for cooling of the plate.
- The Lorentz force opposes the motion of the fluid more effectively in the absence of the Darcian resistance.
- The porosity drag force reduces the skin frictions for a conducting fluid. This suggests that the presence of Darcian resistance reduces the frictional drag at the plate.

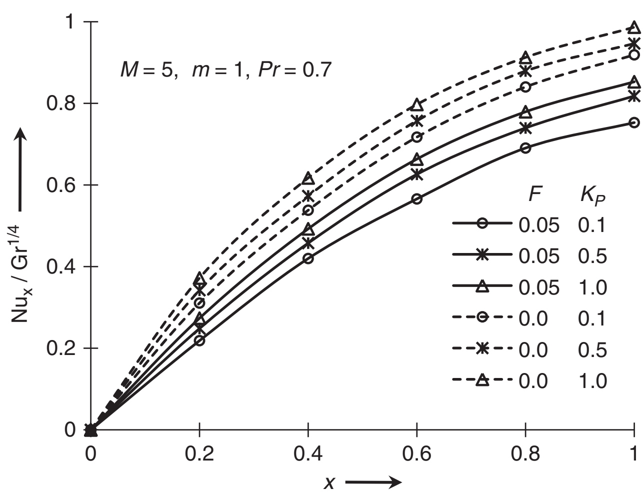

Figure 12.
The effect of radiation-conduction and Darcian drag force on local Nusselt number

- Both the velocity and temperature are strongly enhanced with an increase in time (t) in the Darcian regime.

The present study was confined to Newtonian fluids. It is hoped that the present results be used as a vehicle for understanding more complex problems dealing with viscoelastic and power-law rheological fluid models.

References

Abd El-Naby, M.A., Elbarbary, E.M.E. and Abdelazem, N.Y. (2003), "Finite difference solution of radiation effects on MHD unsteady free-Convection flow over vertical plate with variable surface temperature", *Journal of Applied Mathematics*, Vol. 2003 No. 2, pp. 65-86.

Ahmed, S. (2008), "Transient three dimensional flow through a porous medium with transverse permeability oscillating with time", *Emirate Journal for Engineering research*, Vol. 13 No. 3, pp. 11-17.

Ahmed, S. (2009), "Three-dimensional Channel flow through a porous medium", *Bulletin of Calcutta Mathematical Society*, Vol. 101 No. 5, pp. 503-514.

Ahmed, S. (2010), "Free convective transient three-dimensional flow through a porous medium oscillating with time in presence of periodic suction velocity", *International Journal of Applied Mathematics and Mechanics*, Vol. 6 No. 11, pp. 1-16.

Ahmed, S. and Kalita, K. (2013a), "Magnetohydrodynamic transient flow through a porous medium bounded by a hot vertical plate in presence of radiation: A theoretical analysis", *Journal of Engineering Physics and Thermophysics*, Vol. 86 No. 1, pp. 31-39.

Ahmed, S. and Kalita, K. (2013b), "Analytical numerical study for MHD radiating flow over an infinite vertical plate bounded by porous medium in presence of chemical reaction", *Journal of Applied Fluid Mechanics*, Vol. 6 No. 4, pp. 597-607.

Ahmed, S. and Zueco, J. (2011), "Modelling of heat and mass transfer in a rotating vertical porous channel with hall current", *Chemical Engineering Communications*, Vol. 198 No. 10, pp. 1294-1308.

Ali, M.M., Chen, T.S. and Armaly, B.F. (1984), "Natural convection radiation interaction in boundary layer flow over horizontal surfaces", *AIAA Journal*, Vol. 22 No. 12, pp. 1797-1803.

Bég, O.A., Takhar, H.S. and Singh, A.K. (2005), "Multi-parameter perturbation analysis of unsteady oscillatory magneto-convection in porous media with heat source effects", *International Journal of Fluid Mechanics Research*, Vol. 32 No. 6, pp. 635-661.

Carrier, G.F. and Greenspan, H.P. (1960), "The time-dependent magnetohydrodynamic flow past a flat plate", *Journal of Fluid Mechanics*, Vol. 7 No. 1, pp. 22-32.

Chamkha, A.J. (1996), "Unsteady hydromagnetic natural convection in a fluid-saturated porous medium channel", *Advanced Filtration and Separation Technology*, Vol. 10, pp. 369-375.

Chamkha, A.J. (2001), "Unsteady laminar hydromagnetic flow and heat transfer in porous channels with temperature-dependent properties", *International Journal of Numerical Methods for Heat and Fluid Flow*, Vol. 11 Nos 5-6, pp. 430-448.

Chamkha, A.J., Ahmed, S. and Aloraier, A. (2010), "Melting and radiation effects on mixed convection from a vertical surface embedded in a non-Newtonian fluid saturated non-Darcy porous medium for aiding and opposing external flows", *International Journal of the Physical Sciences*, Vol. 5 No. 7, pp. 1212-1224.

Chamkha, A.J., Takhar, H.S. and Bég, O.A. (2004), "Radiative free convective non-Newtonian fluid flow past a wedge embedded in a porous medium", *Int. J. Fluid Mechanics Research*, Vol. 31 No. 2, pp. 101-115.

Cogley, A.C., Vincenti, W.G. and Gilles, S.E. (1968), "Differential approximation for radiation transfer in a non-gray near equilibrium", *AIAA J*, Vol. 6 No. 3, pp. 551-553.

Ganesan, P., Loganathan, P. and Soundalgekar, V.M. (2001), "Radiation effects on flow past an impulsively started plate", *Int. J. Applied Mechanics Engineering*, Vol. 6 No. 3, pp. 719-730.

Ghaly, A.Y. and Elbarbary, E.M.E. (2002), "Radiation effect on MHD free-convection flow of a gas at a stretching surface with a uniform free stream", *J. Appl. Math*, Vol. 2 No. 2, pp. 93-103.

Ghosh, S.K. and Ḿeg, O.A. (2008), "Theoretical analysis of radiative effects on transient free convection heat transfer past a hot vertical surface in porous media", *Nonlinear Analysis: Modelling and Control*, Vol. 13 No. 4, pp. 419-432.

Ghosh, S.K. and Pop, I. (2007), "Thermal radiation of an optically thin gray gas in the presence of indirect natural convection", *Int. J. Fluid Mechanics Research*, Vol. 34 No. 6, pp. 515-520.

Gupta, A.S. (1960), "Steady and transient free convection of an electrically conducting fluid from a vertical plate in the presence of a magnetic field", *Applied Scientific Research*, Vol. 9 No. 1, pp. 319-333.

Hoffman, J.D. (1992), *Numerical Methods for Engineers and Scientists*, McGraw-Hill, New York, NY.

Hossain, M.A., Rees, D.A.S. and Pop, I. (1998), "Free convection-radiation interaction from an isothermal plate inclined at a small angle to the horizontal", *Acta Mechanica*, Vol. 127 Nos 1-4, pp. 63-73.

Ingham, D.B. and Pop, I. (Eds) (1998), *Transport Phenomena in Porous Media*, Pergamon, Oxford.

Kakac, S. and Yener, Y. (1998), *Convective Heat Transfer*, CRC Press, Boca Raton, FL.

Mohammadein, A.A., Mansour, M.A., El Gaied, S.M. and Gorla, R.S.R. (1998), "Radiative effect on natural convection flows in porous media", *Transport Porous Media*, Vol. 32 No. 3, pp. 263-283.

Muthucumaraswamy, R. and Ganesan, P. (1998), "Unsteady flow past an impulsive by started vertical plate with heat and mass transfer", *Heat and Mass Transfer*, Vol. 34 Nos 2-3, pp. 187-193.

Nield, D.A. and Bejan, A. (2006), *Convection in Porous Media*, 3rd ed., Springer, New York, NY.

Pop, I. (1969), "Unsteady hydromagnetic free convection flow from a vertical infinite flat plate", *Zeitschrift für Angewandte Mathematik und Mechanik*, Vol. 49 No. 12, pp. 756-757.

Prasad, V.R., Reddy, N.B. and Muthucumaraswamy, R. (2006), "Transient radiative hydromagnetic free convection flow past an impulsively started vertical plate with uniform heat and mass flux", *Theoretical Applied Mechanics*, Vol. 33 No. 1, pp. 31-63.

Raptis, A. and Massalas, C.V. (1998), "Magnetohydrodynamic flow past a plate by the presence of radiation", *Heat and Mass Transfer*, Vol. 34 Nos 2-3, pp. 107-109.

Raptis, A. and Perdikis, C. (2004), "Unsteady flow through a highly porous medium in the presence of radiation", *Transport Porous Media J.*, Vol. 57 No. 2, pp. 171-179.

Rohsenow, W.M., Hartnett, J.P. and Cho, Y.I. (Eds) (1998), *Handbook of Heat Transfer*, McGraw-Hill, New York, NY.

Roming, M.F. (1964), "The influence of electric and magnetic fields on heat transfer to electrically conducting fluid", in Irvine T.F. and Hartnett, J.P. (Eds), *Advances in Heat Transfer*, Vol. 1, Academic Press, New York, NY, pp. 286-354.

Seddeek, M.A. (2001), "Thermal radiation and buoyancy effects on MHD free convective heat generating flow over an accelerating permeable surface with temperature dependent viscosity", *Canad. J. Phys*, Vol. 79 No. 4, pp. 725-732.

Shercliff, J.A. (1965), *A Textbook of Magnetohydrodynamics*, Pergamon, Oxford.

Shih, T.M. (1984), *Numerical Heat Transfer*, Series in Computational Methods in Mechanics and Thermal Sciences Hemi-sphere, Washington, DC.

Siegel, R. and Howell, J.R. (1993), *Thermal Radiation Heat Transfer*, Hemisphere, New York, NY.

Soundalgekar, V.M. (1981), "Finite difference analysis of transient free convection with mass transfer on an isothermal vertical flat plate", *Internat. J. Engrg. Sci.*, Vol. 19 No. 6, pp. 757-770.

Takhar, H.S., Gorla, R.S.R. and Soundalgekar, V.M. (1996), "Radiation effects on MHD free convection flow of a gas past a semi-infinite vertical plate", *Internat. J. Numer. Methods Heat Fluid Flow*, Vol. 6 No. 2, pp. 77-83.

Takhar, H.S., Bég, O.A., Chamkha, A.J., Filip, D. and Pop, I. (2003), "Mixed radiation-convection boundary layer flow of an optically dense fluid along a vertical flat plate in a non-Darcy porous medium", *Int. J. Applied Mechanics Engineering*, Vol. 8 No. 3, pp. 483-496.

Takhar, H.S., Ganesan, P., Ekambavahar, K. and Soundalgekar, V.M. (1997), "Transient free convection past a semi-infinite vertical plate with variable surface temperature", *Int. J. Numer. Methods Heat Fluid Flow*, Vol. 7 No. 4, pp. 280-296.

Vadasz, P. (2008), *Emerging Topics in Heat and Mass Transfer in Porous Media*, Springer, New York, NY.

Vafai, K. (2005), *Handbook of Porous Media*, 2nd ed., Taylor and Francis, Boca Raton, FL.

Zueco, J. (2007), "Network simulation method applied to radiation and viscous dissipation effects on MHD unsteady free convection over vertical porous plate", *Applied Mathematical Modelling*, Vol. 31 No. 9, pp. 2019-2033.

Further reading

Ahmed, S. and Kalita, K. (2012), "A sinusoidal fluid injection/suction on MHD three-dimensional Couette flow through a porous medium in the presence of thermal radiation", *Journal of Energy Heat and Mass Transfer* (in press).

Corresponding author

Dr Sahin Ahmed can be contacted at: heat_mass@yahoo.in